# SELECTION OF MATERIALS FOR TARGET STATION EQUIPMENT AT CYCLOTRON CYCLON-70*

E.N. Savitskaya[†], M.A. Maslov, S.A. Nikitin, V.N. Peleshko, N.V. Skvorodnev,
Institute for High Energy Physics of the National Research Centre "Kurchatov Institute"
(NRC KI – IHEP), Protvino, Moscow Region, Russia

## Abstract

A Radioisotope Centre of Nuclear Medicine for commercial production of radioisotopes is under construction now in Protvino. It is based on IBA (Belgium) Cyclone-70 proton cyclotron with proton energy up to 70 MeV and beam current up to 750 µA. The proton beam is split into two halves to provide simultaneous operation of two target stations. NRC KI – IHEP develops the design of the target station to produce nuclides Sr82 and Ge68 by the 70 MeV proton beam with current up to 375µA ($2.3 \cdot 10^{15}$ proton/s).

The present work is devoted to selection of target station materials to minimize the induced radioactivity of equipment during isotopes production. The main source of this radioactivity is a flux of secondary neutrons created from proton-nuclear interactions with target materials. The nucleon-nucleus interactions and the transport of particles in substances were simulated by package of Monte Carlo codes HADR99 and FAN15 specially adapted for this task. Time dependence of the activity of nuclides accumulated in surrounding equipment and the effective dose rate after the end of bombardment (EOB) was calculated. Several alloys were considered and aluminum alloy AMg2 was chosen as most promising base material.

## INTRODUCTION

The wide use of radioactive isotopes in medical practice needs the increase of their industrial production. The manufacturing of radioisotopes Sr82 and Ge68 by the 70 MeV proton beam with current up to 375µA will be organized in Protvino on the base of cyclotron Cyclone-70 (IBA). Sr82 and Ge68 will be generated by irradiating rubidium (or RbCl) and gallium respectively. Wide peak in cross section of reaction $^{nat}Rb(p,xn)^{82}Sr$ lies in the energy range 40 – 70 MeV. The energy range of maximum yield of reaction $^{nat}Ga(p,xn)^{68}Ge$ is 12 – 30 MeV. This makes it possible to irradiate the rubidium and gallium targets simultaneously.

In general, terms the target station is a pipe with bottom inserted into a vertical protective sleeve of transport shaft from the top floor. A guide is installed in the pipe. A carriage moves along the guide by means of a chain connected to the motor. The encapsulated targets are delivered by the carriage to the place of irradiation. On the side of the beam in the pipe there is a window with a thin membrane. The pipe is filled with water. Water serves both the target cooler and neutron shield in the transport shaft. The components of the target station are shown in Fig. 1.

The targets fixed in a duralumin holder will be irradiated for one session (10-14 days). Secondary neutrons from proton-nuclear interactions in target materials have a large penetrating power. Inelastic interactions of neutrons with nuclei of surrounding equipment lead to the accumulation of radionuclides in them. The holder will be disposed of after each session. The remaining details of the target station will be irradiated during a large number of sessions with short technological breaks between them. During the breaks the decline in activity of the details will occur mainly due to the decay of short-lived nuclides. Long-lived nuclides will be accumulated in the materials from the session to the session.
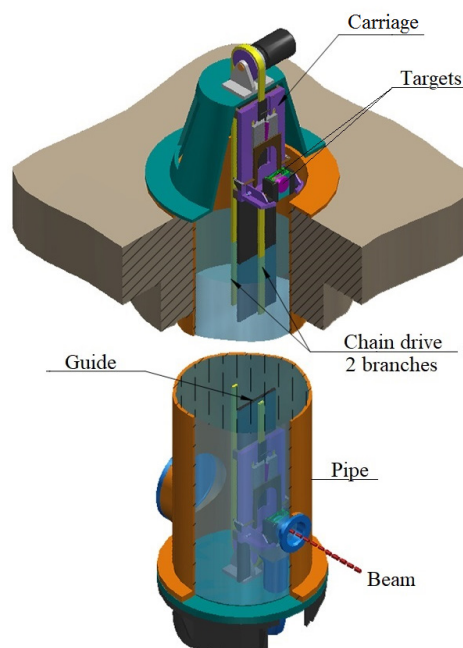


Figure 1: The target station.

Photons, electrons and positrons from nuclide decays form a radiation field in a target hall after the EOB. Photons make the main contribution to the dose rate. Maintenance of the target station involves periodic replacement of the membrane. Therefore, it is required to minimize the induced radioactivity of equipment and to determine what time is necessary for the decay of short-lived nuclides.

## CALCULATION MODEL

The interactions of neutrons and protons with nuclei and the transport of particles in substances are simulated by package of Monte Carlo codes HADR99 [1] and FAN15 [2, 3]. A cascade-exciton model is used to describe the inelastic reactions of neutrons with energy above 20 MeV and protons. The interactions of neutrons ranging

in energy from thermal to 20 MeV with nuclei are simulated in the group approximation. The group cross sections and group-to-group transfer coefficients were calculated from data in the ENDF/B-VI neutron library.

A large number of radionuclides are formed as a result of nuclear interactions of primary protons and secondary protons and neutrons in targets and surrounding equipment. The activity of the nuclide of the i-th type, accumulated during the time $T_0$, decreases with time $T_1$ after the EOB exponentially.

$$A_i(T_0, T_1) = Iw_i(1 - exp(-\lambda_i T_0))exp(-\lambda_i T_1),$$
$$\lambda_i = ln2/T_{1/2}^i$$

where $I$ is the beam current; $w_i$ is the radionuclide yield in the entire volume of the detail, normalized to one primary proton; $\lambda_i$ and $T_{1/2}^i$ are the decay constant and the half-life for the radionuclide.

The contribution $w_{ij}$ to the value of $w_i = \sum_j w_{ij}$ from the interactions of protons with nuclei of the j-th type in matter is determined in the approximation of continuous slowing down by the formula

$$w_{ij} = \frac{\xi_j \; \rho \; N_A}{\sum \xi_j A_j} \int_{E_2}^{E_1} \frac{\sigma_{ij}(E)}{dE/dz} dE \; ;$$

the neutron contribution is

$$w_{ij} = \frac{\xi_j \; \rho \; N_A}{\sum \xi_j A_j} \sigma_{ij}(E) L$$

where $\xi_j$ is the fraction of j-type nuclei with atomic weight $Aj$ in matter; $\rho$ is the matter density; $N_A$ is the Avogadro number; $\sigma_{ij}(E)$ is cross section for production of the i-th nuclide; $dE/dz$ is linear energy transfer in MeV/cm; $E_1$ and $E_2$ are the proton energy at the beginning and the end of the proton trajectory in the detail volume; L is the length of neutron path in the detail volume.

The calculated cross sections $\sigma_{ij}(E)$ were corrected taking into account the experimental values available in the database EXFOR [4].

Gamma radiation from decays of nuclides in activated materials is the main source of the effective dose in the target hall. At a distance R from an activated object, the contribution of the i-th nuclide to the effective dose rate is

$$\dot{E}_\iota(T_0, T_1) = \frac{A_i(T_0, T_1)}{4\pi R^2} \sum_k p_k(E_k^\gamma) \cdot e(E_k^\gamma)$$

Where $p_k(E_k^\gamma)$ is a yield of gamma rays with energy $E_k^\gamma$ per decay of the nuclide from [5]; $e(E_k^\gamma)$ is conversion coefficient from fluence to the effective dose for antero-posterior geometry of irradiation [6]. This formula is applicable if the distance R is much larger than the geometric dimensions of the region of material activation.

## RESULTS AND ANALYSIS

The pipe, carriage, guide and chain were first supposed to be made of stainless steel grade 12X18H10T. Its composition is shown in Table 1.

The calculated geometry includes a part of the pipe with all the contents enclosed between two horizontal planes located 30 cm below and above the beam. Displacement of

these planes at a distance of 50 cm above and below the beam leads to an increase in the activity of details by 1-1.5%. Thus, the overwhelming majority of radionuclides in the pipe, the chain and the guide are located near the beam. From Fig. 2 it can be seen that the carriage and the pipe are subject to greater activation.

Table 1. Chemical Composition of Steel 12X18H10T

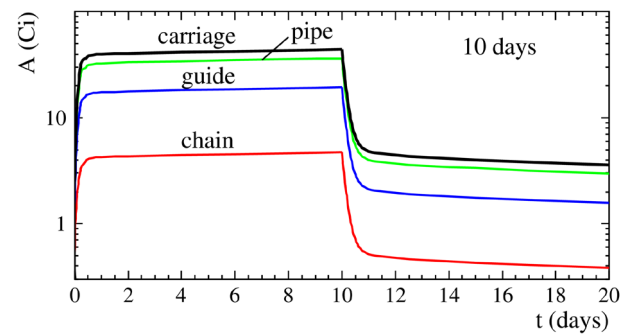| Element | % | Element | % |
|---|---|---|---|
| C | 0.12 | Cr | 18. |
| Si | 0.8 | Mn | 2. |
| P | 0.035 | Fe | 67.925 |
| S | 0.02 | Ni | 10. |
| Ti | 0.8 | Cu | 0.3 |



Figure 2: Activity of the steel target station components during 10 days irradiation and 10 days after the EOB.
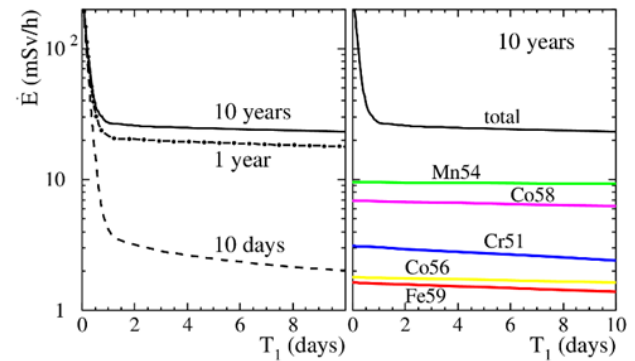


Figure 3: The effective dose rate at 1 m from steel carriage after irradiation during 10 days, 1 year, 10 years (left picture) and contribution of the MLLN to the dose rate after 10 years (right picture).

The activity of the main long-lived nuclides (MLLN) approaches saturation during the first year of irradiation. Therefore, the effective dose rate of photons after one year and ten years of irradiation are close (see Fig. 3 left picture). A couple of days after the EOB Mn54 and Co58 give the most significant contributions to the dose (see Fig. 3 right picture). Nuclide Co58 is formed from the interactions of neutrons with nickel. The highest yield of Mn54 is provided by interactions of neutrons with iron nuclei. Since iron predominates in all steels (more than 60%), then the dose rate will be of the same order of magnitude for other

steel grades. The remaining activated parts of the target station will increase the dose rate at least twice. Consequently, the induced activity will not allow carrying out repair and service in the target hall with the involvement of personnel. Therefore, it became necessary to consider lighter alloys based on aluminum. Calculations were carried out for four alloys based on aluminum: AMg2, AMg6, EN AW-AlMg4.5Mn0.7 (C250) and EN AW-AlZn5.5Mg1.5 (C330), whose chemical composition is given in Table 2.

Table 2. Chemical Composition of Aluminum Alloys AMg2, AMg6, C250 and C330.

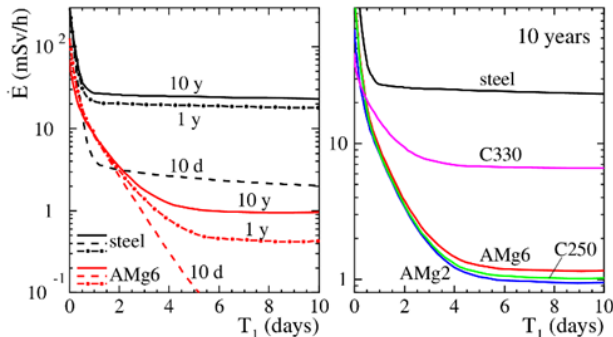| Alloy | AMg2 | AMg6 | C250 | C330 |
|---|---|---|---|---|
| Be | – | 0.003 | – | – |
| Mg | 2.05 | 6.3 | 4.45 | 1.5 |
| Al | 96.95 | 91.787 | 94.05 | 92.305 |
| Si | 0.2 | 0.4 | 0.2 | 0.125 |
| Ti | 0.075 | 0.06 | 0.075 | 0.05 |
| Cr | 0.025 | – | 0.15 | 0.025 |
| Mn | 0.3 | 0.75 | 0.7 | 0.05 |
| Fe | 0.25 | 0.4 | 0.2 | 0.2 |
| Cu | 0.075 | 0.1 | 0.05 | 0.125 |
| Zn | 0.075 | 0.2 | 0.125 | 5.5 |
| Zr | – | – | – | 0.12 |



Figure 4: The effective dose rate at 1 m from carriage after irradiation during 10 days, 1 year, 10 years for steel and AMg6 (left picture) and for all alloys after 10 years (right picture).

It can be seen from Fig. 4 that aluminum alloys create a significantly lower radiation background than steel. Advantage up to 24 times with AMg2 alloy. AMg2, AMg6 and C250 are close in composition, so they are close in the effective dose rate. Alloy C330 contains significantly more zinc. Zn65 is mainly obtained as a result of (n,γ)-reaction. Figure 5 shows that this nuclide gives the largest contribution to the dose for C330 alloy. Na22 is the MLLN for the remaining alloys. It's product of Al(n,x) and Mg(n,x) reactions. The decay of short-lived nuclides in Al-alloys occurs in 6 days after the EOB. Na24 determines this time interval.

Unfortunately, not all the details of the target station can be made from Al-alloys. However, the aluminum pipe, the carriage and possibly part of the guide will reduce the dose rate in the target hall several times.
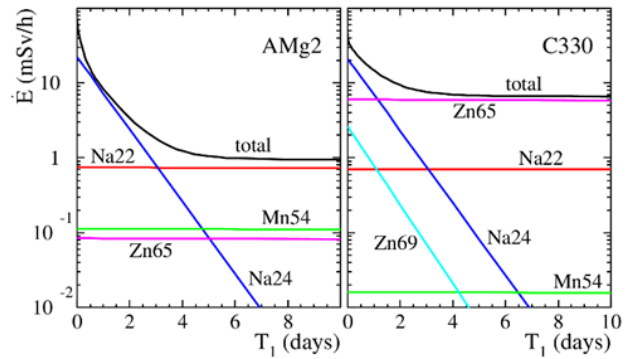


Figure 5: Contribution of the MLLN to the effective dose rate at 1 m from carriage after 10 years for Amg2 (left picture) and c330 (right picture) alloys.

It is also preferable to use aluminum alloys for the equipment of accelerators of high-energy charged particles, since above 100 MeV the cross section for the formation of Na22 by protons and neutrons on Al is practically constant up to 20 GeV and is about 10 mb. Above 30 MeV among the products of nucleon-nuclear reactions, Be7 ($T_{1/2}$ = 53.22 days) appears. Its cross section slowly grows, approaching a maximum value of the order of 8 mb at the energy of about 2 GeV and then it varies little. In decay of Be7 one photon with energy 477.6 keV is emitted with a probability of 10.44%. Therefore, its contribution to the dose rate will be small. In the list of reaction products on Al and Mg there are two more long-lived isotopes: Be10 ($T_{1/2}$=1.51·10$^6$ years) and C14 ($T_{1/2}$ =5700 years). Both do not produce photons in its decay.

## CONCLUSION

It was shown that for the minimization of equipment induced radioactivity on the proton accelerators the aluminum alloys are preferable. In neutron fields with a significant contribution of thermal neutrons, the alloys with low zinc content should be chosen. The effective dose rate from short-lived nuclides in Al-alloys becomes negligible in 6 days after the end of irradiation.

## REFERENCES

[1] Sannikov A.V., Savitskaya E.N. Nucl. Instrum. Meth. Phys. Res., 2000, v. A450, p. 127–137.

[2] Savitskaya E.N. and Sannikov A.V. Atomic Energy, Vol. 122, No. 1, May, 2017 (Russian Original Vol. 122, No. 1, January, 2017).

[3] Savitskaya E.N. and Sannikov A.V. Atomic Energy, Vol. 122, No. 2, June, 2017 (Russian Original Vol. 122, No. 2, February, 2017).

[4] https://www-nds.iaea.org/

[5] http://www.nndc.bnl.gov/nudat2/

[6] ICRP, 2010. Conversion Coefficients for Radiological Protection Quantities for External Radiation Exposures. ICRP Publication 116, Ann. ICRP 40(2–5).